KI REPORTS
KIReports.org
TRANSLATIONAL RESEARCH

Flow-Cytometric Quantification of Urine Kidney Epithelial Cells Specifically Reflects Tubular Damage in Acute Kidney Diseases

Leonie Wagner[1,2,11], Jacob Kujat[1,2,11], Valerie Langhans[1,2,11], Luka Prskalo[1,2], Diana Metzke[1,2], Emil Grothgar[1,2], Paul Freund[2], Nina Goerlich[1,2,9], Hannah Brand[2], Sara Timm[3], Matthias Ochs[3,4,5], Andreas Grützkau[2], Sabine Baumgart[2,6], Christopher M. Skopnik[1,2], Adrian Schreiber[1,10], Falk Hiepe[2,7], Gabriela Riemekasten[8], Philipp Enghard[1,2,11] and Jan Klocke[1,2,9,11]

[1]Department of Nephrology and Medical Intensive Care, Charité-Universitätsmedizin Berlin, corporate member of Freie Universität Berlin and Humboldt-Universität zu Berlin, Berlin, Germany; [2]Deutsches Rheumaforschungszentrum, an Institute of the Leibniz Foundation, Berlin, Germany; [3]Core Facility Electron Microscopy, Charité-Universitätsmedizin Berlin, corporate member of Freie Universität Berlin and Humboldt-Universität zu Berlin, Berlin, Germany; [4]Institute of Functional Anatomy, Charité-Universitätsmedizin Berlin, corporate member of Freie Universität Berlin and Humboldt-Universität zu Berlin, Berlin, Germany; [5]German Center for Lung Research, Berlin, Germany; [6]Institute for Immunology/Core Facility Cytometry, Jena University Hospital, Jena, Germany; [7]Department of Rheumatology, Charité Universitätsmedizin, Berlin, Germany; [8]Department of Rheumatology, University of Lübeck, Lübeck, Germany; [9]Berlin Institute of Health at Charité - Universitätsmedizin Berlin, BIH Biomedical Innovation Academy, BIH Charité Clinician Scientist Program, Berlin, Germany; and [10]Experimental and Clinical Research Center, Max Delbrück Center for Molecular Medicine, Berlin, Germany

Introduction: Tubular injury is one of the main mechanisms driving acute kidney injury (AKI); however, clinicians still have a limited diagnostic repertoire to precisely monitor damage to tubular epithelial cells (TECs). In our previous study, we used single-cell sequencing to identify TEC subsets as the main components of the urine signature of AKI. This study aimed to establish TECs as clinical markers of tubular damage.

Methods: A total of 243 patients were analyzed. For sequencing, we collected 8 urine samples from patients with AKI and glomerular disease. We developed a protocol for the flow cytometric quantification of CD10/CD13$^+$ proximal TECs (PTECs) and CD227/CD326$^+$ distal TECs (DTECs) in urine by aligning urinary single-cell transcriptomes and TEC surface proteins using Cellular Indexing of Transcriptome and Epitope Sequencing (CITE-Seq). Marker combinations were confirmed in kidney biopsies. We validated our approach in 4 cohorts of 235 patients as follows: patients with AKI ($n = 63$), COVID-19 infection ($n = 47$), antineutrophil cytoplasmic autoantibody (ANCA)–associated vasculitis (AAV) with active disease or stable remission ($n = 110$), and healthy controls ($n = 15$).

Results: Our findings demonstrated that CD10/CD13 and CD227/CD326 adequately identified PTECs and DTECs, respectively. Distal urinary TEC counts correlate with the severity of AKI based on Kidney Disease: Improving Global Outcomes (KDIGO) stage and acute estimated glomerular filtration rate (GFR) loss in 2 separate cohorts and can successfully discriminate AKI from healthy controls and glomerular disease.

Conclusion: We propose that urinary CD227/CD326$^+$ TEC count is a specific, noninvasive marker for tubular injury in AKI. Our protocol provides a basis for a deeper phenotypic analysis of urinary TECs.

Kidney Int Rep (2025) **10,** 1260–1273; https://doi.org/10.1016/j.ekir.2025.01.037
KEYWORDS: acute kidney injury; ANCA-associated vasculitis; flow cytometry; single-cell sequencing; tubular epithelial cells; urinalysis

AKI affects up to 20 % of hospitalized patients and is associated with increased morbidity and mortality.[1,2] Damage to kidney TECs is a key feature of AKI, and the most prominent histopathological and transcriptional changes because of AKI are found in the TEC-compartment.[3,4] However, damage and loss of TECs are not unique features of AKI, but also occur in other kidney diseases, albeit to a lesser extent.

To date, clinicians have a limited diagnostic repertoire to monitor damage to the kidney tubular epithelium. Traditionally, functional tests such as fractional

Correspondence: Jan Klocke, Department of Nephrology and Medical Intensive Care, Charité Universitätsmedizin Berlin, Chariteplatz 1, 10117 Berlin, Germany. E-mail: jan.klocke@charite.de

[11]LW, JKu, VL, PE, and JKI contributed equally

Received 3 July 2024; revised 3 December 2024; accepted 27 January 2025; published online 3 February 2025

excretion of sodium or urea have been employed, despite being of limited use.[5] Several novel biomarkers for AKI have been developed that reflect tubular stress (TIMP-2 and IGFBP-7 [Nephrocheck]),[6,7] tubular damage or injury (neutrophil gelatinase–associated lipocalin,[8,9] and kidney injury molecule 1[10]) or activation of a local immune reaction (IL-18,[8] CCL-14[11]); however, wide application of these new markers in clinical routine is pending.

An alternative and potentially more direct approach to measure stress and damage to the kidney tubular epithelium is the quantification of TECs in urine. Detection of TECs and cell casts via urine microscopy is a well-established marker for AKI and "acute tubular necrosis".[12,13] Moreover, high amounts of renal TECs or cell casts in urine have been associated with the need for dialysis,[14] probability of nonrecovery,[15] and adjusted odds of worsening AKI and sepsis.[16] The use of microscopy is impaired by a lack of objectivity because of low interobserver reliability, lack of clinician experience, and time constraints in modern clinical practice.[17]

We recently used single-cell sequencing to demonstrate that TEC subtypes originating from different parts of the nephron can be found in the urine, alongside other kidney and immune cells.[18] Here, we translated these findings and developed a flow cytometry (FC)–based quantification of PTECs and DTECs, based on a detection protocol derived from single-cell gene and protein expression data via CITE-seq. FC-based analysis of urinary TECs offers the advantages of precise quantification, cost-effectiveness, and the opportunity to easily extend the analysis to other TEC subtypes to monitor AKI and predict its outcome. Using our FC-based analysis of urinary TECs, we analyzed patients with AKI, COVID-19, AAV, and healthy cohorts to demonstrate its clinical utility.

METHODS

Urine Single-Cell Sequencing and Data Analysis

For scRNA-seq, urine samples were collected from 8 patients with kidney disease. Five patients had impaired kidney perfusion or tubular necrosis because of myocardial infarction ($n = 2$), successful resuscitation ($n = 2$), or septic shock ($n = 1$). Samples were taken 2 to 10 days after the hit. To guarantee the necessary viable cell counts, these AKI samples were pooled into groups of 3 and measured in 2 rounds. One patient was included in both pools (days 2 and 10 after hit). Two patients with primary glomerular diseases, refractory membranous nephropathy ($n = 1$) and active proliferative lupus nephritis (class IV) ($n = 1$), were also included. For more detailed information (Table 1).

Table 1. Characteristics of single cell analysis cohort

Characteristics	sc
n	8
Age, yr	
Mean	62.38
SD	18.88
Range	29–81
Sex, n (%)	
Male	6
Female	2
Baseline SCr (mg/dl)	
Mean	0.8
SD	0.12
Range	0.7–1.1
SCr on day of measurement (mg/dl)	
Mean	1.8
SD	0.69
Range	0.9–3.0
AKI	
STEMI	2
PE + ROSC	2
ARDS	1
MGN	1
LN	1
No AKI	1
Chronic kidney disease, n (%)	
Yes	3
No	5

AKI, acute kidney injury; ARDS, acute respiratory distress syndrome; KDIGO, Kidney Disease: Improving Global Outcomes; LN, lupus nephritis; MGN, membranous glomerular nephritis; PE, pulmonary embolism; ROSC, return of spontaneous circulation; Sc, single cell; SCr, serum creatinine; STEMI, ST-Elevation myocardial infarction.
Values are mean (range).

Samples were processed and analyzed as described previously[18] and incubated with Totalseq B hashtag antibodies for CD10, CD13, and CD326 (BioLegend). Hashtag oligo libraries were added to the Seurat object as an independent assay and normalized ("NormalizeData [SO, assay = "HTO, "normalization.method = "CLR"]"). To ensure a high cluster resolution and detection of low abundant cell types, datasets were integrated with our urine AKI single-cell transcriptome dataset published previously[18] after quality control for downstream analysis [*"SCTransform()", "RunPCA(dims=1:45)", "RunHarmony()", "RunUMAP()", "FindNeighbors()", "FindClusters()"*]. Single-cell data were a subset of the newly acquired dataset.

Patients

A total of 243 patients were included as follows: 8 patients for single-cell sequencing and 235 patients for FC analysis. For FC, we collected and analyzed urine samples from 63 patients with AKI, 47 with COVID-19, 110 with AAV, and 15 controls for urine FC analysis. Causes of AKI were adjudicated based on available records (sepsis, $n = 15$; cardiac event, $n = 22$; postsurgery, $n = 11$; other, $n = 15$) and patients with suspected glomerulonephritis or acute interstitial

Table 2. Characteristics of AKI cohort

Characteristics	Control group	AKI group 1	AKI group 2	AKI group 3
n	15	35	13	15
Age, yr				
Mean	58.5	70.3	68.9	65.8
SD	19.0	11.9	15.7	11.4
Range	24–89	40–86	34–84	36–80
Sex, n (%)				
Male	7 (47%)	26 (74%)	10 (77%)	7 (47%)
Female	8 (53%)	9 (26%)	3 (23%)	8 (53%)
Baseline SCr (mg/dl)	-			
Mean		0.94	0.91	0.68
SD		0.20	0.23	0.22
Range		0.55–1.38	0.53–1.42	0.33–1.31
SCr on day of measurement (mg/dl)	-			
Mean		1.30	1.67	2.53
SD		0.29	0.56	1.93
Range		0.78–2.02	0.53–2.62	0.75–7.72
Etiology of AKI, n (%)	-			
Cardiac event		16 (46%)	2 (15%)	4 (27%)
Septic		2 (6%)	6 (46%)	7 (46%)
Multifactorial		17 (48%)	5 (38%)	4 (27%)
Chronic kidney disease, n (%)	-			
Yes		10 (29%)	2 (15%)	1 (7%)
No		25 (71%)	11 (85%)	14 (93%)
MAKE-30	-			
Yes		6 (17%)	3 (23%)	7 (47%)
No		29 (83%)	10 (77%)	8 (53%)

AKI, acute kidney injury; KDIGO, Kidney Disease: Improving Global Outcomes; MAKE-30, major adverse kidney events within 30 days of AKI onset.; SCr, serum creatinine.
Values are mean (range).

Table 3. Characteristics of COVID-19 cohort

Characteristics	Control group	AKI group 1	AKI group 2	AKI group 3
n	25	6	4	12
Age				
Mean	56	72.7	62	63.5
SD	11.8	11.4	5.9	13.7
Range	34–80	55–86	54–67	33–78
Sex, n (%)				
Male	17 (68%)	4 (67%)	4 (100%)	8 (67%)
Female	8 (32%)	2 (33%)	0 (0%)	4 (33%)
Baseline SCr (mg/dl)				
Mean	0.73	1.27	0.84	0.99
SD	0.12	0.84	0.21	0.69
Range	0.5–0.9	0.68–2.88	0.71–1.15	0.50–3.0
SCr on day of measurement (mg/dl)				
Mean	1.2	1.56	1.93	2.56
SD	0.14	1.2	0.36	1.41
Range	0.59–1.4	0.86–3.9	1.54–2.39	0.98–5.12
Chronic kidney disease, n (%)				
Yes	0 (0%)	2 (33%)	0 (0%)	1 (8%)
No	23 (92%)	4 (67%)	4 (100%)	11 (92%)
Na	2 (8%)	0 (0%)	0 (0%)	0 (0%)
Clinical deterioration				
Yes	5 (20%)	2 (33%)	2 (50%)	10 (83%)
No	20 (80%)	4 (67%)	2 (50%)	2 (17%)

SCr, serum creatinine.
Values are mean (range).

nephritis were excluded. We refer to this cohort as the AKI cohort throughout the paper, and patients with ANCA-associated AKI are discussed separately. Patients with urinary tract infections or postrenal AKI, as well as children and kidney transplant patients, were excluded from the analysis. All samples were collected within 72 hours of the onset of kidney damage and examined using FC. All patients were classified according to their maximum KDIGO stage within 72 hours after AKI onset (referred to as KDIGO groups "1," "2," or "3"). Whenever available, urine output was used along with serum creatinine (SCr) values for AKI classification. All SCr values, including follow-up data, were retrieved from the electronic medical records. SCr levels were measured using the Jaffé method. Renal recovery was defined according to the definition of AKI as renormalization of the SCr below a value 1.5 times the baseline value or below the baseline value plus 0.3 mg/dl, depending on the AKI sub-definition used for study subject inclusion. Major adverse kidney events, MAKE-30, were defined as persistently impaired kidney function, need for new renal replacement therapy, or in-hospital mortality within 30 days of AKI onset. The characteristics of patients with AKI are shown in Table 2.

In the COVID-19 cohort, 47 patients were included, of whom 22 presented with AKI at the time of sampling and 6 additional patients developed AKI in the following week. Sixteen patients experienced clinical deterioration, according to World Health Organization guidelines.[19] Clinical deterioration was defined as progression in disease severity, mainly the worsening of respiratory symptoms or radiographic findings.[20] Twenty-eight patients in this cohort were treated in the intensive care unit at the time of sampling, with continuous monitoring of urinary output. COVID-19 positive patients without AKI served as controls. The patient characteristics are shown in Table 3.

For AAV, we included 3 cohorts consisting of patients with active disease ($n = 20$), inactive disease with renal involvement ($n = 74$), and without renal involvement ($n = 16$). Remission was defined as a Birmingham Vasculitis Activity Score of 0, regardless of prednisone use. The inclusion criteria were patients diagnosed with AAV according to the Chapel-Hill consensus definition, those who had been in remission (Birmingham Vasculitis Activity Score = 0) for a minimum of 3 months and those aged 18 years or older.

Table 4. Characteristics of AAV cohort

Characteristics	Stable disease with renal involvement	Stable disease without renal involvement	Active disease
n	74	16	20
Age, yrs			
Mean	63.1	65.5	56.2
SD	12.4	15.4	14.5
Range	30–86	36–83	25–85
Sex, n (%)			
Male	43 (58%)	5 (31%)	15 (75%)
Female	31 (42%)	11 (69%)	5 (25%)
Baseline SCr (mg/dl)			
Mean	1.75	1.2	1.37
SD	0.87	0.08	0.81
Range	0.59–5.23	0.58–1.3	0.60–4.30
SCr on day of measurement (mg/dl)	-	-	
Mean			2.26
SD			1.91
Range			0.70–8.40
Chronic kidney disease, n (%)			
yes	67 (91%)	7 (44%)	17 (85%)
no	7 (9%)	9 (56%)	3 (15%)
KDIGO stage of AKI			
no AKI	74 (100%)	16 (100%)	9 (45%)
1			4 (20%)
2			1 (5%)
3			6 (30%)

AKI, acute kidney injury; KDIGO, Kidney Disease: Improving Global Outcomes; SCr, serum creatinine.
Values are mean (range).

Patients exhibiting persistent proteinuria or hematuria for more than 3 months before study enrollment were classified as inactive based on the Birmingham Vasculitis Activity Score V3 definition.[21–23] Active disease was defined as a Birmingham Vasculitis Activity Score $\geq$ 1 point.[24] Exclusion criteria encompassed concurrent urinary tract infection or active menstrual bleeding. The characteristics of patients with AAV are shown in Table 4.

The control group consisted of 5 healthy individuals without previous renal impairment and 10 in-patients without current renal impairment. Because there was no difference in urine cell counts between both groups, they are presented jointly as "healthy controls." More information is presented in Table 2.

Written informed consent was obtained from all patients before their participation in the study. Renal and ureteral tissue samples were obtained from deceased patients, and written consent was obtained from their relatives. Ethical approval was obtained from the Ethics Committee of Charité University Hospital (Charité EA1/239/16, EA1/284/19, EA2/141/19, and EA2/045/18). The study was conducted in accordance with the ethical guidelines of the Declaration of Helsinki and our institution.

Tissue Staining

We established a staining protocol for urinary PTECs and DTECs using human postmortem renal and ureteral tissue samples. Four kidney samples and 1 ureter sample were stored in Gibco Roswell Park Memorial Institute 1640 Medium (Thermo Fisher Scientific, Waltham, MA) containing 10% fetal calf serum and 1% penicillin/streptomycin and digested using collagenase VIII (1.5 mg/ml, Serva Electrophoresis GmbH, Heidelberg, Germany) and DNAse I (50µg/ml, Roche, Basel, Switzerland). The staining protocol and antibodies used correspond to the urine staining protocol described below.

Sample Preparation and FC

After collection, the urine samples were immediately centrifuged and washed in phosphate-buffered saline containing 0.5% bovine serum albumin and 2 mM ethylenediaminetetraacetic acid (Thermo Fisher Scientific, Waltham, MA). The approximate standing time for the urine samples before preparation was 3 to 6 hours. First morning void urine samples were preferentially used. In the handling of the AAV cohorts, a urine-cup-based fixation system with imidazolidinyl urea (Sigma-Aldrich) and 3-(N-morpholino) propanesulfonic acid (MOPS, Carl Roth GmbH + Co. KG) to preserve urine samples[25] was used. Specimen were stored at 4 °C for up to 7 days, centrifuged (600 g, 6 minutes) and frozen in 90% fetal calve serum and 10% dimethylsulfoxide (cohort 1 and 3). Before conducting our analysis, we defrosted samples in phosphate-buffered saline, pH 7.2 with 0.2 % bovine serum albumin and 2 mM ethylenediaminetetraacetic acid and strained through a 30 µm cell strainer (Miltenyi Biotech). For cytokeratin staining, the cells were fixed using 4% paraformaldehyde and subsequently perforated using a perm/wash solution (confirmatory cohort; BD Biosciences, Franklin Lakes, NJ). The cells were resuspended in phosphate-buffered saline/bovine serum albumin containing 10% human IgG (Flebogamma; Grifols, Langen, Germany) to block nonspecific binding. Afterward, staining with antibodies was carried out by incubation for 20 minutes at 4 °C in the dark. The complete staining protocol included pan-cytokeratin-APC (clone: REA831; isotype: recombinant human IgG1) or, exclusively for fluorescence microscopy, pan-cytokeratin-FITC (clone: CK3-6H5; isotype: mouse IgG1), CD13-PE (clone: REA263; isotype: recombinant human IgG1), CD10-PE-Vio770 (clone: 97C5; isotype: mouse IgG1), CD326-PE (clone: HEA-125; isotype: mouse IgG1), and CD227-PE-Vio770 (clone: REA448; isotype: recombinant human IgG1) (all Miltenyi Biotec GmbH, Bergisch Gladbach, Germany).

Samples were filtered immediately before analysis using MACS preseparation filters with a mesh size of 70 μm. If cell sorting before microscopic examination was performed, a mesh size of 30 μm was used (Miltenyi Biotec GmbH, Bergisch Gladbach, Germany). Stained samples were processed using a BD FACSCanto II and BD LSRFortessa flow cytometer (BD Biosciences, Franklin Lakes, NJ). Final analysis was performed using FlowJo Software (Tree Star, Ashland, OR). The calculated cell numbers were normalized to a volume of 100 ml urine.

Microscopy

The samples were prepared as described above and subsequently purified using a Sony MA900 multiapplication cell sorter (Sony Group Corporation, Minato, Tokyo, Japan). The resulting cell suspension was sorted directly on a polysine adhesion slide (Thermo Fisher Scientific, Waltham, MA), dried at room temperature in the dark, and mounted with ProLong Diamond Antifade Mountant solution (Thermo Fisher Scientific, Waltham MA). A Keyence BZ-9000 Biorevo fluorescence microscope (Keyence, Osaka, Japan) equipped with DAPI and GFP filters was used for fluorescence imaging. No additional staining was observed during this process. Basic image processing, including cropping, brightness or contrast adjustment, and gamma correction, was performed using ImageJ 1.53 k software.

For electron microscopic analysis, cells were fixed with 2.5 % glutaraldehyde in 0.1 M sodium cacodylate buffer for 30 minutes at room temperature and stored at 4 °C. Before electron microscopic analysis, the DTECs were isolated using FC-based sorting. As CD326 was denatured during the fixation process, the cells were stained only for cytokeratin, DAPI, and CD227. Based on our FC data, the analyzed urine samples almost never contained CD227+ cell populations that stained negative for CD326. The samples were postfixed with 1% osmium tetroxide (Electron Microscopy Sciences, Hatfield, PA) and 0.8 % potassium ferrocyanide II (Roth, Karlsruhe, Germany) in 0.1 M cacodylate buffer for 1.5 hours and pelleted in agarose overnight. After dehydration in a graded ethanol series, samples were embedded in Epon resin (Roth, Karlsruhe, Germany). Finally, the ultrathin sections (70 nm) were stained with uranyl acetate and lead citrate. The examination was carried out using a Zeiss 906 electron microscope (Carl Zeiss, Oberkochen, Germany) at an acceleration voltage of 80 kV, equipped with a slow-scan 2K CCD camera (TRS, Moorenweis, Germany).

Statistical Analysis

Because the TEC counts were not normally distributed, they were log10 transformed. Differences in TEC counts between subgroups of the AKI cohort were tested using analysis of variance or *t* tests. For multiple group comparisons, *t* tests were used as *post hoc* tests. Differences in TEC counts between the subgroups of the ANCA cohort were tested using Welch's *t* test. For comparison of TEC counts between different cohorts, the Kruskal-Wallis test and Wilcoxon rank-sum test for *post hoc* analysis were used. Assumptions were tested statistically and visually using the Shapiro-Wilk test, Levene's test, QQ plots, and boxplots. Confidence intervals for receiver operator characteristic curve analyses were calculated using bootstrapping with 2000 stratified bootstrap replicates.[26] Cut-off values corresponding to the optimal trade-off between sensitivity and specificity were determined using Youden's index. To test the influence of age, biological sex, and the presence of chronic kidney disease on TEC count, subgroup analyses were carried out for all patients in the AKI and ANCA cohorts, using Spearman correlation and *t* tests. For all analyses, the significance level was set to $\alpha = 0.05$. Alpha error inflation was corrected using the Bonferroni-Holm correction. All analyses were performed using R Studio 2022.07.2,[27] rstatix package[28] and the pROC package.[29]

RESULTS

Singe-Cell Sequencing-Based Validation of Markers to Detect Urinary TECs Using FC

Single-cell transcriptomes allow for unbiased detection and clustering of urinary cells, and we previously reported the detection of TECs of proximal and distal origin by marker gene expression. To establish an FC-based marker panel for the detection of defined urinary cell populations, we first determined the surface marker expression patterns of renal cells excreted in the urine. We used a tandem approach to analyze single-cell transcriptomes and surface antigen expression using barcode-tagged antibodies (CITE-seq) in 8 urine samples. We compared transcriptomic signatures from tissue[4] and urine,[18] with urine cell surface signatures for markers previously used in flow cytometric detection of TECs as follows: CD10/MME and CD13/ANPEP for PTECs and CD326/EpCAM for DTECs.[30,31]

A total of 7575 single-cell transcriptomes from 8 patient urine samples were analyzed after quality control (Figure 1a and f). To ensure better identification of low-abundance cell types, we integrated the data with our previously published urine AKI single-cell transcriptome dataset published previously.[18] Cell clusters were identified by marker gene expression; for

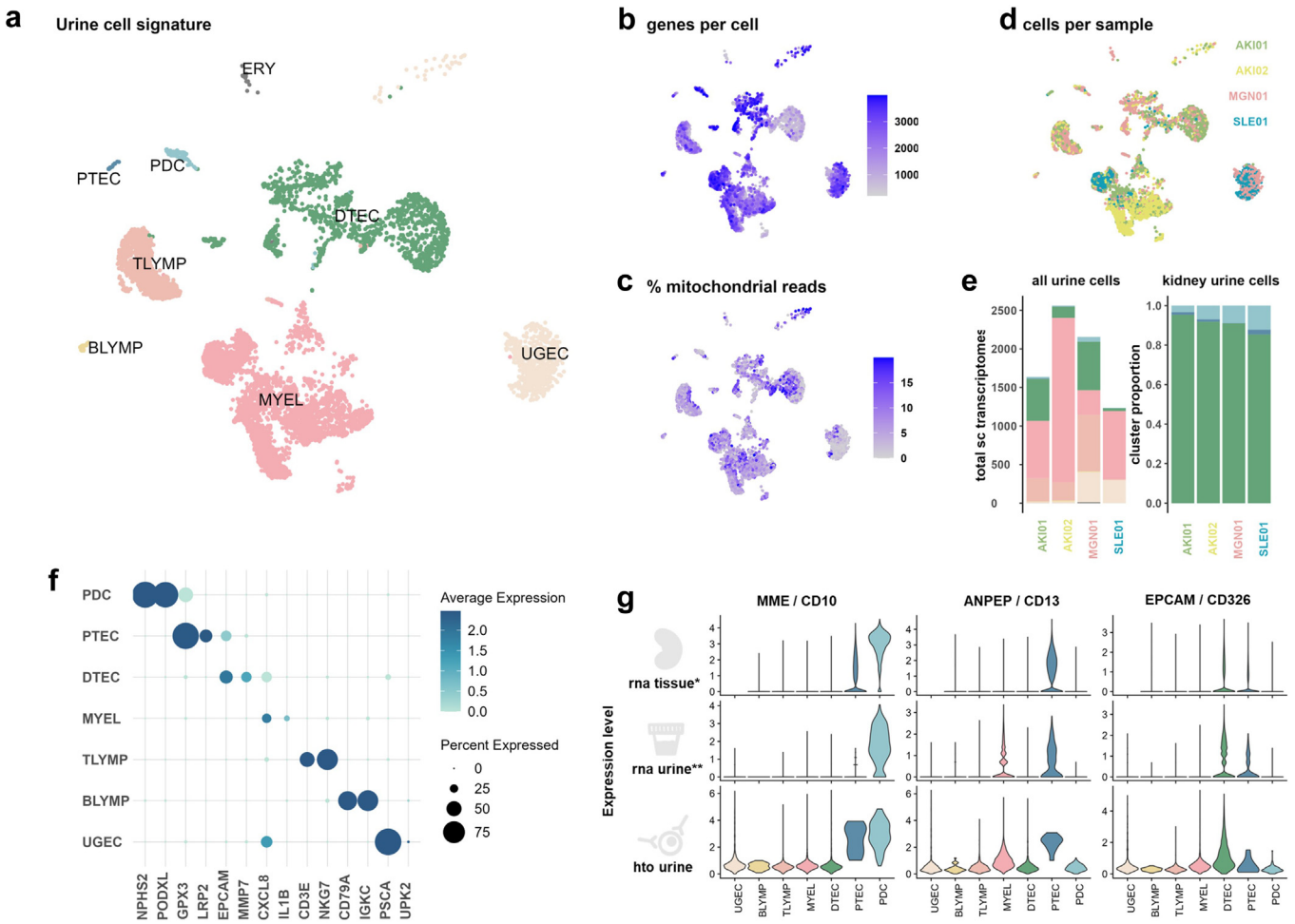

Figure 1. CITEseq in urinary single-cell sequencing shows loss of CD10 in urine. (a) Uniform manifold approximation and projection (UMAP) of 7575 single-cell RNA-sequencing urine cells from 7 individuals with AKI ($n = 5$), MGN ($n = 1$) and LN ($n = 1$). Cellular composition is individually diverse but can be broadly grouped into kidney cells (podocytes [PDCs] and distal and proximal tubular epithelial cells [DTECs or PTECs]), urogenital epithelial cells (UGECs), myeloid cells (MYEL), B and T lymphocytes (B/T LYMPHs) and erythrocytes (ERYs). (b–d) Quality control: Distribution of cells in UMAP by (b) genes per cell, (c) mitochondrial reads and (d) individual distribution. (e) Individual distribution of total transcriptomes and urinary cluster proportions. Irrespective of disease, predominantly DTECS and myeloid cells are found. (f) Dot plot of marker gene expression for each cell type. (g) RNA expression of CD10/MME, CD13/ANPEP, and CD326/EPCAM in tissue and urine and respective hashtag oligos in urine. CD326 is exclusively expressed on DTECs, CD13 on PTECs and myeloid cells, and CD10 is continuously expressed on podocytes. PTECs lose CD10 RNA expression in urine compared with tissue, while surface antigen markers stay positive. AKI, acute kidney injury; LN, lupus nephritis; MGN, membranous glomerular nephritis.

example, the PTEC cluster of cells had high expression of the marker gene, *LRP2* (Figure 1a and f). The overall sample quality was high, with a median of 1553 genes/cell and 4283 reads/cell, and an even distribution of cell types and clusters across the different samples (Figure 1b–d).

As seen in our previous study, TEC clusters comprised mostly distal and dedifferentiated phenotypes, with only a small subset of PTECs (Figure 1e). Further information regarding the DTEC subgroups is available in our previous study.[18]

Next, we compared the transcriptome and corresponding protein signatures to validate the TEC markers for FC, which showed that concerning PTEC marker, CD10 was detectable on the cell surface, although transcription of the corresponding gene, *MME*, was depleted in urine than in tissue (Figure 1g). In addition to PTECs, podocytes were CD10^{+}, which correlated with a high transcriptomic signature in both tissue and urine podocytes. CD13/ANPEP was detectable mostly in PTECs but also in a subset of myeloid cells. Coexpression of CD10 and CD13 was uniquely found in PTECs, although these cells had very low abundance in urine. DTEC clusters were considerably more heterogeneous in terms of their transcriptomic phenotype but exclusively transcribed EPCAM and surface-expressed CD326 in our urine dataset (Figure 1g).

To substantiate the use of these surface antigen markers for FC, we validated our findings using

postmortem kidney biopsies ($n = 4$) as positive controls and ureter tissue ($n = 1$) as a negative control. Although CD10 and CD13 in combination adequately identified proximal tubular cells, we found that the DTEC marker CD326 was also expressed in ureter cells. To increase specificity, we added CD227 to our DTEC marker panel, which was not found in ureter cells (Figure 2b and c). Using these marker combinations, we sorted urine cells for fluorescence microscopic analysis. Isolated CK/CD13/10$^+$ and CK/CD227/326$^+$ cells from the urine of patients with AKI showed typical TEC morphology on fluorescence microscopy (Figure 2e–f). Electron microscopy of purified urinary CK/CD227$^+$ cells from patients with AKI revealed a predominant fraction of apoptotic and necrotic cells within the sorted cell population, including morphological characteristics such as chromatin condensation at the nuclear periphery, rounded cell shape, apoptotic bodies, loss of cell membrane integrity, vacuolization, and karyopyknosis. The TECs in unsorted urine samples demonstrated similar features, ruling out the induction of these changes during cell isolation (Figure 2g–j).

Urinary TECs Correlate With Severity of AKI

To establish urinary TECs as biomarkers in patients with tubular injury, we recruited 235 patients from 4 separate cohorts. Patient details, including the clinical etiology of AKI, are presented in Tables 2 to 4. The samples were analyzed by FC and normalized to 100 ml of urine. Exemplary dot plots illustrating distinct TEC populations are shown in Figure 2a to d.

Our primary AKI cohort mainly consisted of patients with prerenal, septic, and multifactorial AKI. Patients with AKI stage 3 had the highest TEC counts (Figure 3a and b). The increase in PTECs in the KDIGO stage 1, 2, and 3 groups only reached significance when compared with the control group (each $P < 0.001$, Figure 3a); whereas for DTECs, all comparisons except for KDIGO stages 2 and 3 were significant ($P < 0.001$, Figure 3b). Accordingly, the maximum acute estimated GFR loss correlated with the PTECs and DTECs counts ($P < 0.001$, Figure 3d and e).Patients with AKI with a major adverse kidney event within 30 days after AKI onset presented with significantly higher urinary DTEC counts at the time of measurement ($t = -2.27$, $P = 0.031$, Supplementary Figure S1D). We found no influence of AKI etiology on the number of urinary TECs (Supplementary Figure S1A–C). To assess the diagnostic ability of PTECs and DTECs in discriminating patients with AKI from controls, we calculated receiver operator characteristic curves (Figure 3c). The areas under the curve for diagnosing AKI using PTEC and DTEC counts were 0.91 and 0.93, respectively. The cutoffs for PTEC and DTEC counts determined by Youden's index and the corresponding sensitivity and specificity are displayed in Figure 3c. Thus, cell counts of both PTECs and DTECs were significantly correlated with the severity of kidney injury.

COVID -19: AKI Validation Cohort

To validate our findings, we measured urinary TECs in 47 hospitalized patients with COVID-19, a collective prone to AKI. PTECs demonstrated significantly poor discrimination between the AKI and control groups and no correlation with GFR loss (Figure 4a and d). In contrast, DTECs continued to perform well in both discrimination and correlation with GFR decline for all KDIGO stages ($P < 0.001$, Figure 4b and e) and were elevated in a small group of patients ($n = 6$) that did not meet the AKI criteria at the point of measurement but developed AKI in the following week. Consistent with the above results, the area under the receiver operator characteristic curve for COVID-AKI were 0.606 for PTECs and 0.855 for DTECs (Figure 4c). Both PTEC and DTEC counts were significantly elevated in patients who showed clinical deterioration in the next 7 days according to the World Health Organization disease stage ($P = 0.025$ / $P < 0.001$, Supplementary Figure S2A and B). Importantly, there was no correlation between diuresis and cell count, implying that the abundance of cells was not related to urine concentration (Supplementary Figure S2C and D).

Urinary TECs in Patients With AAV

Having demonstrated that urinary TECs reflect kidney damage in AKI, we assessed urinary TECs in patients with AAV. To this end, 3 cohorts of patients with AAV were included as follows: 1 with active AAV and 2 cohorts of patients in stable remission, both with and without renal involvement. We did not find a significant difference in the number of TECs between active AAV, inactive AAV with renal involvement, and inactive AAV without renal involvement (Figure 5a and c). A comparison with routine clinical data revealed a correlation between albuminuria and the number of TECs in active disease, although only PTECs showed a significant increase (Figure 5b and d). Interestingly, in patients with stable disease, no correlation was observed between PTECs or DTECs and albuminuria (Figure 6b and d). Furthermore, urinary TECs did not correlate with the current chronic kidney disease stage in patients with stable AAV or with changes in the GFR slope in the subsequent six months (Supplementary Figure S3A and D). To rule out different therapeutic regimens as confounding factors, we integrated current immunosuppressive treatments into our analysis. Compared with patients without treatment, azathioprine and rituximab were associated

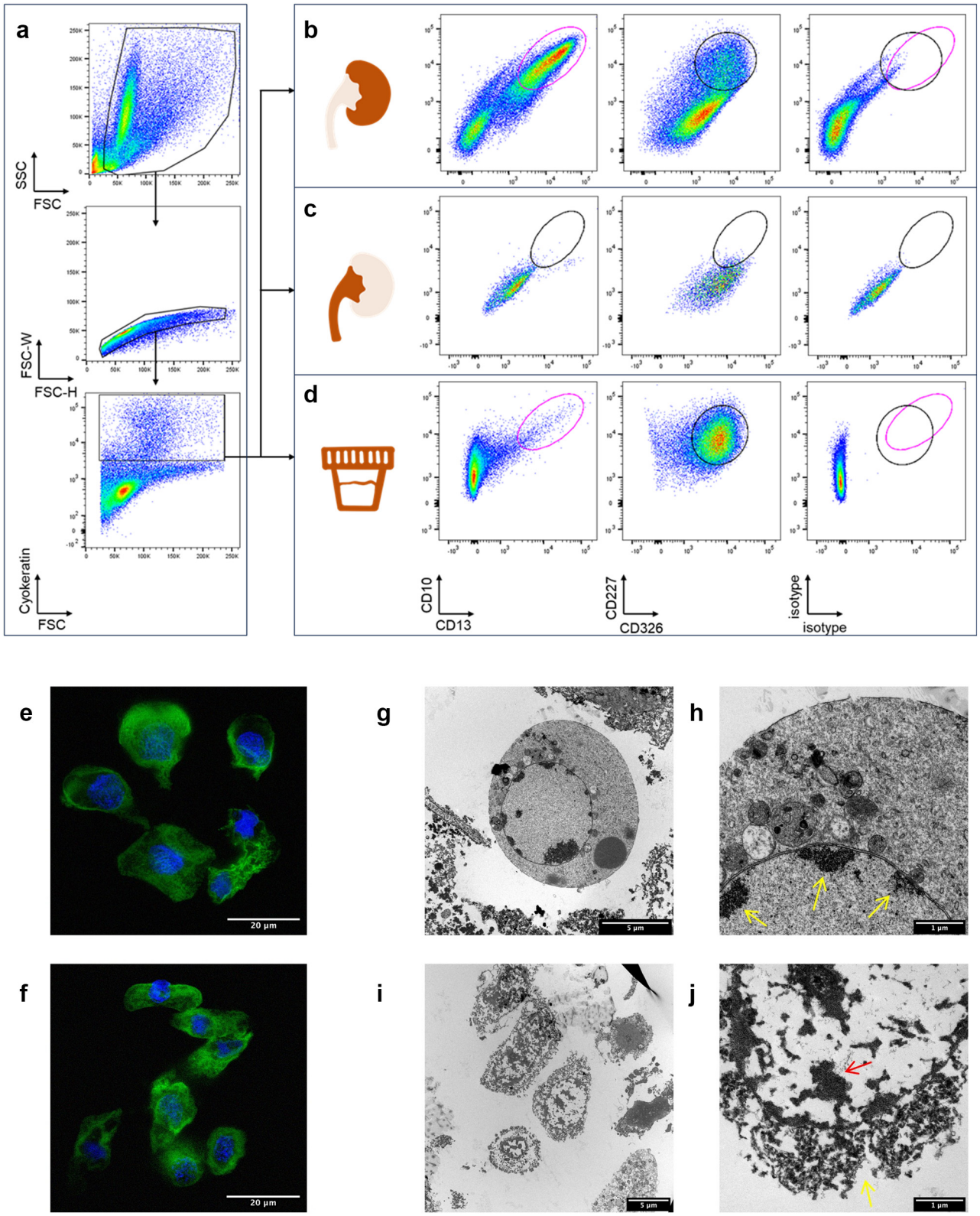

Figure 2. The amount of urinary TECs can be measured using flow cytometry. (a) Gating strategy for selecting cytokeratin positive single cells. Staining of CD10, CD13, CD326, and (b) CD227 compared with isotype-controls in postmortem kidney tissue, (c) postmortem ureteral tissue, and (d) urine. Note CD326 but not CD227 positivity in ureteral epithelial cells. (e,f) Fluorescence microscopic image of (e) purified CK+DAPI+CD13+CD10+ cells, and (f) purified CK+DAPI+CD326+CD227+ cells (blue = DAPI, green = cytokeratin). (g–j) Electron microscopic images of purified cytokeratin+CD227+ cells using a cell sorter. (g and detail h) Apoptotic cell with characteristic marginalization of condensed chromatin (yellow arrows in h) and intact plasma membrane. (i and j) Necrotic cells with chromatin clumping (red arrow in j) and loss of plasma membrane integrity as distinguishing feature from apoptosis (yellow arrow in j). TECs, tubular epithelial cells.

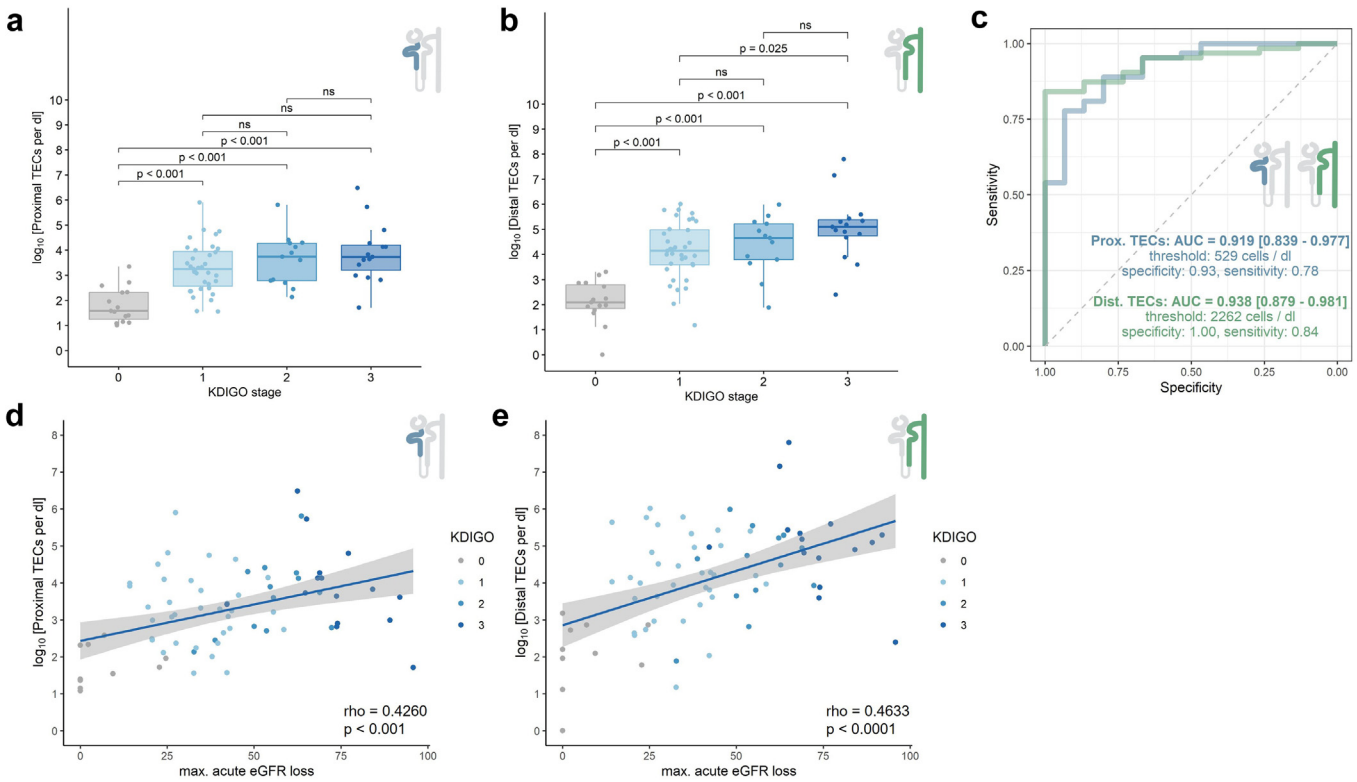

Figure 3. Flow cytometric quantification of proximal and distal TEC counts in patients with AKI. (a and b) (a) Proximal and (b) distal TEC counts shown for different KDIGO stages. (c) Receiver operator characteristic (ROC) curve for distinguishing AKI from healthy and inpatient controls. Area under the curve (AUC). Cut-offs for proximal and distal TEC counts were determined by Youden's index. (d and e) Correlation of (d) proximal and (e) distal TECs and the maximal loss of eGFR during the course of AKI. AKI, acute kidney injury; eGFR, estimated glomerular filtration rate; TEC, tubular epithelial cell

with a significantly lower number of PTECs, whereas for DTECs, only rituximab showed lower cell counts (Supplementary Figure S3B and E).

Urinary TECs Discriminate AKI From Glomerular Damage

To assess whether urinary TECs can be used as discriminatory markers for different kidney damage patterns, we directly compared patient cohorts. Patients with AKI, regardless of the underlying cause, exhibited significantly higher DTEC counts than patients with AAV and controls(H[2] = 71.30, $P < 0.001$; *post hoc* analysis: AKI vs. AAV, $P < 0.001$; AKI vs. COVID controls, $P < 0.001$; AKI vs. healthy controls, $P < 0.001$; AKI vs. COVID-AKI, not significant; Figure 6a and b). Urinary DTEC counts effectively identified patients from both AKI cohorts when compared with controls and patients with AAV (the area under the receiver operator characteristic curve: 0.83, Figure 6c). In the subgroup analyses of patients from the AKI and AAV cohorts, no influence of age (AKI cohort, $P = 0.291$; AAV cohort, $P = 0.388$) or the presence of chronic kidney disease (AKI cohort,$P = 0.570$; AAV cohort, $P = 0.445$) on total urinary TEC counts was observed. In contrast, TEC counts were higher in female patients with AAV ($P = 0.003$) than in male patients with AAV. The sex of the patients had no influence on the TEC counts in patients in the AKI cohort ($P = 0.110$, data not shown).

Taken together, urine TEC quantity can discriminate patients with nonautoimmune AKI from those with AAV and no tubular damage. In all cohorts, DTEC counts were significantly higher than PTEC counts. Thus, urine DTECs are markers of tubular stress and are correlated with the extent of kidney injury.

DISCUSSION

This study established the use of flow cytometric urinalysis of CD326/CD227^{+}TECs as a new marker of tubular kidney damage.

Urine scRNA-seq expands the possibilities of urine sediment analysis by providing very detailed information about urinary cells, thereby amplifying its diagnostic potential.[32] Still, sequencing is cost- and time-intensive, and the analysis remains demanding. FC may be ideal for translating this standardized and objective approach to urine cell analysis into a widely available and scalable tool. In the current dataset, CITEseq examination of urine cell clusters helped define surface marker panels to be used in urine FC

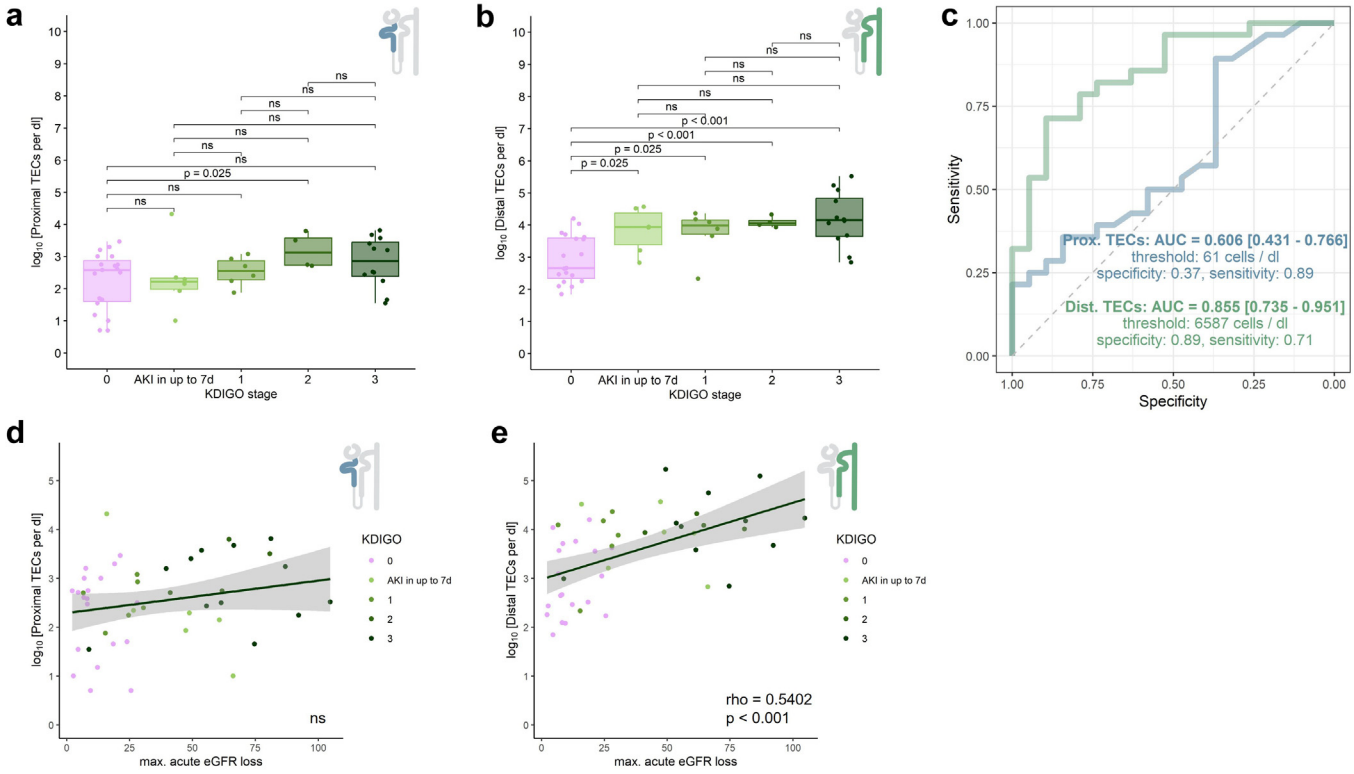

Figure 4. Flow cytometric quantification of proximal and distal TEC counts in patients with COVID-19–AKI. (a and b) (a) Proximal and (b) distal TEC counts shown for different KDIGO stages and patients who develop AKI in the next 7 days. (c) Receiver operator characteristic (ROC) curve for distinguishing AKI from in-patient controls. Area under the curve (AUC). Cut-offs for proximal and distal TEC counts were determined by Youden's index. (d and e) Correlation of (d) proximal (d) and (e) distal TECs and the maximal loss of eGFR during the course of AKI. AKI, acute kidney injury; dTEC, distal tubular epithelial cell; eGFR, estimated glomerular filtration rate; KDIGO, Kidney Disease: Improving Global Outcomes; pTEC, proximal tubular epithelial cell.

analysis. We show that CD10/CD13 is a surface marker combination specific for a low abundant urine TEC subset of the proximal tubule. CD326, in combination with CD227, can be used as a global TEC marker in urine, encompassing the distal tubular segments and dedifferentiated TECs.[18]

Translating urine scRNA-seq findings to FC-based analysis posed 2 major challenges. First, the inconsistent correlation of gene transcription and protein expression was addressed by CITEseq. Interestingly, we found that the CD10 corresponding gene neprilysin (*MME*), was not transcribed in urinary PTECs; however, CD10 was still expressed on the surface. In lung and brain tissues, the protein expression of neprilysin is diminished after episodes of hypoxia; however, whether this concept is transferable to the kidney remains to be elucidated.[33-36] Second, in scRNA-seq, only viable cells are captured and measured, whereas our current flow cytometric approach does not distinguish between cell states and viability. This leads to a discrepancy between counts in both methods, with FC being the gold standard for the quantification of cell populations.[37] Because urinary amounts of PTEC counts determined by FC are higher than measured with scRNAseq, we believe that most of the detected PTECs in urine are already apoptotic or dead. Low overall cell counts in single-cell samples and the uncertainty of CD10 expression, combined with the inherent noisiness of urine FC data, make it difficult to recommend urine CD10/CD13^{+} PTECs as a reliable marker for tubular damage, especially in our COVID-19 cohort. Because CD227/CD326^{+} DTEC counts aligned better between our methods and encompassed a large fraction of urine-excreted TECs, we considered it to be a more robust marker.

In our AKI cohort, we found PTECs as well as DTECs to correlate well with the severity of AKI and consequently with the occurrence of MAKE-30 events. The extent of the injury appeared to be proportional to the number of TECs. In COVID-19 AKI, the correlation between TEC count and kidney injury prevails, although it is less pronounced. The high number of patients in the intensive care unit allowed us to continuously measure urine output to validate our TEC counts with respect to diuresis. Establishing urinary biomarkers in AKI is challenging because of variable urine creatinine excretion and fluctuating expression of renal creatinine transporters, making it difficult to

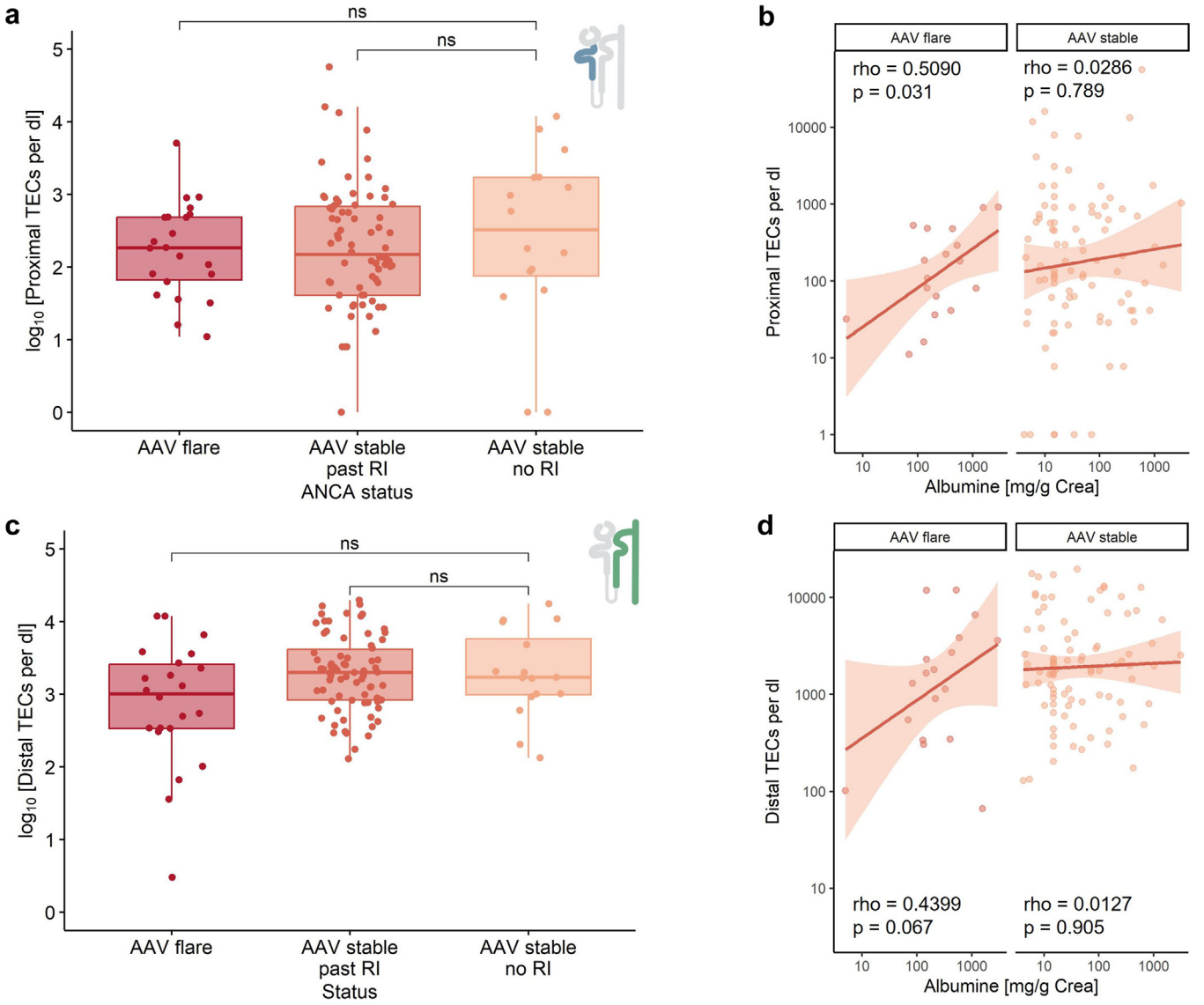

Figure 5. Flow cytometric quantification of proximal and distal TEC counts in patients with AAV. (a and c) (a) Proximal and (c) distal TEC counts in active and stable disease with and without renal involvement. (b and d) (b) Proximal and (d) distal TEC counts in active and stable disease in correlation with albuminuria. AAV, antineutrophil cytoplasmic autoantibody (ANCA)–associated vasculitis; AAV flare, active disease; AAV stable, inactive disease; TEC, tubular epithelial cells

determine threshold values for normalized biomarkers.[38–40] To this extent, we could rule out a concentration effect in the direct measurement of TEC counts by showing that there is no correlation between urine output and TEC abundance.

In line with these findings, we found that TEC counts were lower in the AAV cohorts and did not correlate with creatinine levels, because the primary injury mechanism was glomerular damage. Notably, the number of PTECs was correlated with albuminuria only in patients with active disease. This likely reflects the tubular damage accompanying glomerular injury in active AAV.[41] Patients with COVID-19 without AKI and patients with inactive AAV showed elevated urine TEC levels and stable proteinuria compared with healthy controls, suggesting ongoing tubular stress. The number of TECs was independent of renal involvement, implying that other factors contributed to the intensified shedding of TECs. Although we found a slight association between lower urine TEC counts and immunosuppressive treatment in these patients, the cause of this constant urine TEC excretion in patients with stable AAV remains unclear. Further phenotyping of urine TEC subsets, focusing on regenerative and maladaptive populations, may help to understand the significance of the observed shedding of TECs and further enhance the prediction of clinical outcomes.

Currently, clinicians lack a standardized method for detecting and quantifying the tubular effects in kidney

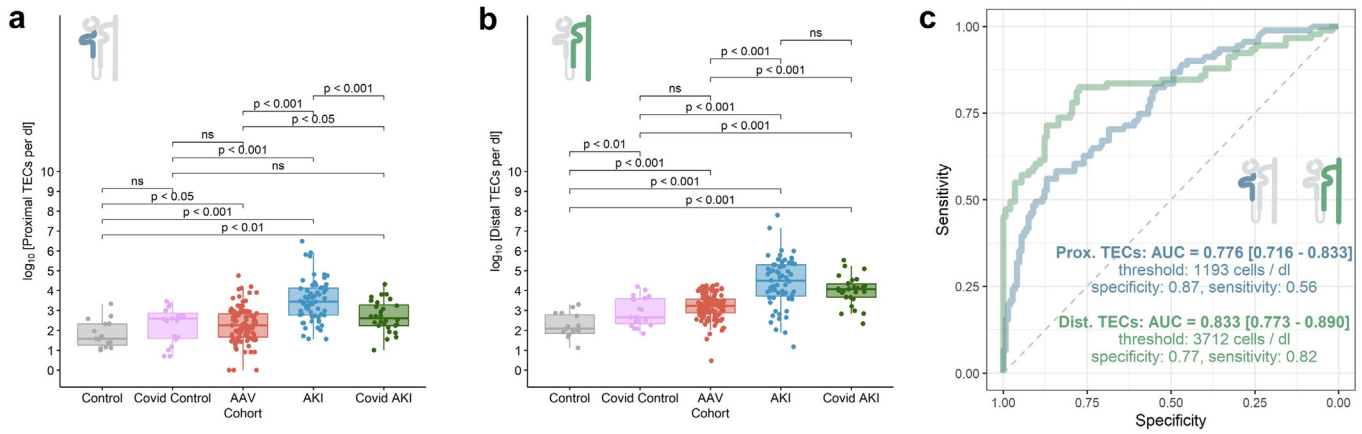

Figure 6. Proximal and distal TECs show differences in renal damage patterns. (a and b) (a) Proximal and (b) distal TECs in healthy controls and different disease entities. (c) Receiver operator characteristic (ROC) curve for distinguishing AKI from healthy and inpatient controls and ANCA-associated vasculitis (AAV). Area under the Curve (AUC). Cut-offs for proximal and distal TEC counts were determined by Youden's index. AKI, acute kidney injury; TEC, tubular epithelial cells.

diseases. Although tubular proteinuria and fractional excretion of sodium or urea may indicate tubular damage, their predictive value for AKI following an insult is limited and restricted to the assessment of the proximal tubule.[42] We now report urinary TEC quantification as a direct correlate of tubular damage.

Limitations

Although our data strongly suggest an association between tubular damage and TEC quantity in the urine, AKI remains a heterogeneous disease with multiple pathomechanisms. Because definitive histological evidence of tubular damage was not available in these cases, we cannot conclusively rule out other potential disease triggers. By assessing our biomarker in relation to SCr, its validity was restricted to biases inherent in creatinine use. In addition, other variables such as comorbidities, intake of nephrotoxic drugs, and initiation of volume therapy need to be taken into consideration. Therefore, a comprehensive kinetic characterization of urine TEC is required.

As evidenced by scRNA-seq urine cell analysis, urine TEC comprise multiple phenotypes, some of which may indicate disease form and severity. Although CD326/EpCAM is a global urine TEC marker (except for low-abundance PTECs), a more nuanced marker panel for distinguishing TEC phenotypes using FC should be established in future studies. Further phenotyping of urinary TECs by complementing the established staining protocol with additional markers of activation, proliferation, senescence, and cell death would provide valuable insights for monitoring kidney function.

CONCLUSION

Quantification of urinary kidney TECs using FC is feasible and enables the direct measurement of tubular damage in patients with AKI. Our findings extend emerging evidence that FC-based urinalysis, especially when combining TECs with markers of renal inflammation such as T cells and monocytes,[30,31,43] can be developed into a standardized renal liquid biopsy.

DISCLOSURE

All the authors declared no competing interests.

ACKNOWLEDGMENTS

This work was supported by grants from the Berlin Institute of Health, the Jackstädt-Stiftung, the Deutsche Forschungsgemeinschaft (DFG; HI 2238/2-1), and Bundesministerium für Bildung und Forschung. JK was supported by a research scholarship from the Deutsche Gesellschaft für Nephrology. We thank the Core Facility for Electron Microscopy of the Charité for support in data acquisition (and analysis) of the data. We thank the Flow Cytometry and Cell Sorting Facility and laboratory managers at DeutschesRheuma-Forschungszentrum Berlin for their technical support and helpful insights. We thank all staff at the Charité's nephrology, cardiology, and intensive care wards for helping with sample collection and all patients for participating.

DATA AVAILABILITY STATEMENT

The sequencing data supporting the findings of this study are available in the Gene Expression Omnibus repository at GSE282344.

AUTHOR CONTRIBUTIONS

JKl and PE designed the study. JKl, CMS, DM, EG, LP, JKu, LW, PF, NG, HB, VL, ST, MO, SB, FH, GR, and PE conducted the experiments and acquired data. JKl, JKu, LW, and PE analyzed the data. JKl, LW, VL, JKu, and PE interpreted the results. JKl, LW, and PE wrote the manuscript.

ADDITIONAL INFORMATION

To review GEO accession GSE282344:

Go to https://www.ncbi.nlm.nih.gov/geo/query/acc.cgi?acc=GSE282344

Enter token otkpgmggrzepvit into the box

SUPPLEMENTARY MATERIAL

Supplementary File (PDF)

Figure S1. Further specification of AKI cohort.

Figure S2. Amount of TECs correlates with clinical deterioration independent of diuresis.

Figure S3. Various influence factors on TEC count in AAV.

REFERENCES

1. Hoste EAJ, Kellum JA, Selby NM, et al. Global epidemiology and outcomes of acute kidney injury. *Nat Rev Nephrol*. 2018;14:607–625. https://doi.org/10.1038/s41581-018-0052-0
2. Cheng X, Wu B, Liu Y, Mao H, Xing C. Incidence and diagnosis of acute kidney injury in hospitalized adult patients: A retrospective observational study in a tertiary teaching Hospital in Southeast China. *BMC Nephrol*. 2017;18:203. https://doi.org/10.1186/s12882-017-0622-6
3. Wen Y, Yang C, Menez SP, Rosenberg AZ, Parikh CR. A systematic review of clinical characteristics and histologic descriptions of acute tubular injury. *Kidney Int Rep*. 2020;5:1993–2001. https://doi.org/10.1016/j.ekir.2020.08.026
4. Hinze C, Kocks C, Leiz J, et al. Single-cell transcriptomics reveals common epithelial response patterns in human acute kidney injury. *Genome Med*. 2022;14:103. https://doi.org/10.1186/s13073-022-01108-9
5. Abdelhafez M, Nayfeh T, Atieh A, et al. Diagnostic performance of fractional excretion of sodium for the differential diagnosis of acute kidney injury: A systematic review and meta-analysis. *Clin J Am Soc Nephrol*. 2022;17:785–797. https://doi.org/10.2215/CJN.14561121
6. Doukas P, Frese JP, Eierhoff T, et al. The NephroCheck bedside system for detecting stage 3 acute kidney injury after open thoracoabdominal aortic repair. *Sci Rep*. 2023;13:11096. https://doi.org/10.1038/s41598-023-38242-2
7. Nalesso F, Cattarin L, Gobbi L, Fragasso A, Garzotto F, Calò LA. Evaluating Nephrocheck(®) as a predictive tool for acute kidney injury. *Int J Nephrol Renovasc Dis*. 2020;13:85–96. https://doi.org/10.2147/IJNRD.S198222
8. Parikh CR, Coca SG, Thiessen-Philbrook H, et al. Postoperative biomarkers predict acute kidney injury and poor outcomes after adult cardiac surgery. *J Am Soc Nephrol*. 2011;22:1748–1757. https://doi.org/10.1681/ASN.2010121302
9. Devarajan P. Neutrophil gelatinase-associated lipocalin: A promising biomarker for human acute kidney injury. *Biomark Med*. 2010;4:265–280. https://doi.org/10.2217/bmm.10.12
10. Han WK, Bailly V, Abichandani R, Thadhani R, Bonventre JV. Kidney Injury Molecule-1 (KIM-1): A novel biomarker for human renal proximal tubule injury. *Kidney Int*. 2002;62:237–244. https://doi.org/10.1046/j.1523-1755.2002.00433.x
11. Hoste E, Bihorac A, Al-Khafaji A, et al. Identification and validation of biomarkers of persistent acute kidney injury: The RUBY study. *Intensive Care Med*. 2020;46:943–953. https://doi.org/10.1007/s00134-019-05919-0
12. Mehta RL, Pascual MT, Soroko S, et al. Spectrum of acute renal failure in the intensive care unit: The Picard experience. *Kidney Int*. 2004;66:1613–1621. https://doi.org/10.1111/j.1523-1755.2004.00927.x
13. Kanbay M, Kasapoglu B, Perazella MA. Acute tubular necrosis and pre-renal acute kidney injury: Utility of urine microscopy in their evaluation- a systematic review. *Int Urol Nephrol*. 2010;42:425–433. https://doi.org/10.1007/s11255-009-9673-3
14. Marcussen N, Schumann J, Campbell P, Kjellstrand C. Cytodiagnostic urinalysis is very useful in the differential diagnosis of acute renal failure and can predict the severity. *Ren Fail*. 1995;17:721–729. https://doi.org/10.3109/08860229509037640
15. Chawla LS, Dommu A, Berger A, Shih S, Patel SS. Urinary sediment cast scoring index for acute kidney injury: A pilot study. *Nephron Clin Pract*. 2008;110:c145–c150. https://doi.org/10.1159/000166605
16. Bagshaw SM, Haase M, Haase-Fielitz A, Bennett M, Devarajan P, Bellomo R. A prospective evaluation of urine microscopy in septic and non-septic acute kidney injury. *Nephrol Dial Transplant*. 2012;27:582–588. https://doi.org/10.1093/ndt/gfr331
17. Wald R, Bell CM, Nisenbaum R, et al. Interobserver reliability of urine sediment interpretation. *Clin J Am Soc Nephrol*. 2009;4:567–571. https://doi.org/10.2215/CJN.05331008
18. Klocke J, Kim SJ, Skopnik CM, et al. Urinary Single-Cell Sequencing Captures Intrarenal Injury and Repair Processes in Human Acute Kidney Injury. *Kidney Int*. 2022;102(6):1359–1370. https://doi.org/10.1016/j.kint.2022.07.032
19. WHO guidelines approved by the guidelines review committee. In: *Clinical Management of COVID-19: Living Guideline*. Geneva: World Health Organization; 2021. Accessed February 14, 2025. https://iris.who.int/bitstream/handle/10665/349321/WHO-2019-nCoV-clinical-2021.2-eng.pdf?sequence=1
20. Wu Z, McGoogan JM. Characteristics of and important lessons from the coronavirus disease 2019 (COVID-19) outbreak in china: Summary of a report of 72314 cases from the Chinese Center for Disease Control and Prevention. *JAMA*. 2020;323:1239–1242. https://doi.org/10.1001/jama.2020.2648
21. Geetha D, Seo P, Ellis C, Kuperman M, Levine SM. Persistent or new onset microscopic hematuria in patients with small vessel vasculitis in remission: Findings on renal biopsy. *J Rheumatol*. 2012;39:1413–1417. https://doi.org/10.3899/jrheum.111608
22. Chen TK, Murakami C, Manno RL, Geetha D. Hematuria duration does not predict kidney function at 1 year in ANCA-associated glomerulonephritis. *Semin Arthritis Rheum*. 2014;44:198–201. https://doi.org/10.1016/j.semarthrit.2014.03.008
23. Magrey MN, Villa-Forte A, Koening CL, Myles JL, Hoffman GS. Persistent hematuria after induction of

remission in Wegener granulomatosis: A therapeutic dilemma. *Medicine*. 2009;88:315–321. https://doi.org/10.1097/MD.0b013e3181c101cc

24. Mukhtyar C, Lee R, Brown D, et al. Modification and Validation of the Birmingham Vasculitis Activity Scoreversion 3. *Ann Rheum Dis*. 2009;68:1827–1832. https://doi.org/10.1136/ard.2008.101279
25. Freund P, Skopnik CM, Metzke D, et al. Addition of formaldehyde releaser imidazolidinyl urea and MOPS buffer to urine samples enables delayed processing for flow cytometric analysis of urinary cells: A simple, two step conservation method of urinary cells for flow cytometry. *Cytom B*. 2023;104:417–425. https://doi.org/10.1002/cyto.b.22117
26. Carpenter J, Bithell J. Bootstrap confidence intervals: When, which, what? A practical guide for medical statisticians. *Stat Med*. 2000;19:1141–1164. https://doi.org/10.1002/(sici)1097-0258(20000515)19:9<1141::aid-sim479>3.0.co;2-f
27. RStudio Team (2022). RStudio: Integrated development for R. RStudio, PBC, Boston, MA. http://www.rstudio.com/
28. Kassambara A, Herviou L, Ovejero S, et al. RNA-sequencing data-driven dissection of human plasma cell differentiation reveals new potential transcription regulators. *Leukemia*. 2021;35:1451–1462. https://doi.org/10.1038/s41375-021-01234-0
29. Robin X, Turck N, Hainard A, et al. pROC: An open-source package for R and S+ to analyze and compare ROC curves. *BMC Bioinformatics*. 2011;12:77. https://doi.org/10.1186/1471-2105-12-77
30. Grothgar E, Goerlich N, Samans B, et al. Urinary CD8+HLA-DR+ T cell abundance non-invasively predicts kidney transplant rejection. *Front Med (Lausanne)*. 2022;9:928516. https://doi.org/10.3389/fmed.2022.928516
31. Goerlich N, Brand HA, Langhans V, et al. Kidney transplant monitoring by urinary flow cytometry: Biomarker combination of T cells, renal tubular epithelial cells, and podocalyxin-positive cells detects rejection. *Sci Rep*. 2020;10:796. https://doi.org/10.1038/s41598-020-57524-7
32. Abedini A, Zhu YO, Chatterjee S, et al. Urinary single-cell profiling captures the cellular diversity of the kidney. *J Am Soc Nephrol*. 2021;32:614–627. https://doi.org/10.1681/ASN.2020050757
33. Kerridge C, Kozlova DI, Nalivaeva NN, Turner AJ. Hypoxia affects neprilysin expression through caspase activation and an APP intracellular domain-dependent mechanism. *Front Neurosci*. 2015;9:426. https://doi.org/10.3389/fnins.2015.00426
34. Carpenter TC, Stenmark KR. Hypoxia decreases lung neprilysin expression and increases pulmonary vascular leak. *Am J Physiol Lung Cell Mol Physiol*. 2001;281:L941–L948. https://doi.org/10.1152/ajplung.2001.281.4.L941
35. Giuliani KTK, Grivei A, Nag P, et al. Hypoxic human proximal tubular epithelial cells undergo ferroptosis and elicit an NLRP3 inflammasome response in CD1c+ dendritic cells. *Cell Death Dis*. 2022;13:739. https://doi.org/10.1038/s41419-022-05191-z
36. Mishra D, Singh S, Narayan G. Role of B cell development marker CD10 in cancer progression and prognosis. *Mol Biol Int*. 2016;2016:4328697. https://doi.org/10.1155/2016/4328697
37. Robinson JP, Roederer M. HISTORY OF SCIENCE. Flow cytometry strikes gold. *Science*. 2015;350:739–740. https://doi.org/10.1126/science.aad6770
38. Tonomura Y, Uehara T, Yamamoto E, Torii M, Matsubara M. Decrease in urinary creatinine in acute kidney injury influences diagnostic value of urinary biomarker-to-creatinine ratio in rats. *Toxicology*. 2011;290:241–248. https://doi.org/10.1016/j.tox.2011.10.001
39. Waikar SS, Sabbisetti VS, Bonventre JV. Normalization of urinary biomarkers to creatinine during changes in glomerular filtration rate. *Kidney Int*. 2010;78:486–494. https://doi.org/10.1038/ki.2010.165
40. Ralib AM, Pickering JW, Shaw GM, et al. Test characteristics of urinary biomarkers depend on quantitation method in acute kidney injury. *J Am Soc Nephrol*. 2012;23:322–333. https://doi.org/10.1681/ASN.2011040325
41. Hakroush S, Tampe D, Korsten P, Ströbel P, Tampe B. Systematic scoring of tubular injury patterns reveals interplay between distinct tubular and glomerular lesions in ANCA-associated glomerulonephritis. *J Clin Med*. 2021;10:2682. https://doi.org/10.3390/jcm10122682
42. Parikh CR, Lu JC, Coca SG, Devarajan P. Tubular proteinuria in acute kidney injury: A critical evaluation of current status and future promise. *Ann Clin Biochem*. 2010;47:301–312. https://doi.org/10.1258/acb.2010.010076
43. Prskalo L, Skopnik CM, Goerlich N, et al. Urinary CD4+ T cells Predict Renal Relapse in ANCA-Associated Vasculitis: Results of the PRE-FLARED Study. *J Am Soc Nephrol*. 2024;35:483–494. https://doi.org/10.1681/ASN.0000000000000311